ISSN 0030-400X, Optics and Spectroscopy, 2008, Vol. 105, No. 1, pp. 25–31. © Pleiades Publishing, Ltd., 2008.
Original Russian Text © A.D. Bykov, N.N. Lavrentieva, T.M. Petrova, L.N. Sinitsa, A.M. Solodov, R. Barber, J. Tennyson, R.N. Tolchenov, 2008, published in Optika i Spektroskopiya, 2008, Vol. 105, No. 1, pp. 31–38.

SPECTROSCOPY OF ATOMS AND MOLECULES

Shift of the Centers of H_2O Absorption Lines in the Region of 1.06 μm

A. D. Bykov[a], N. N. Lavrentieva[a], T. M. Petrova[a], L. N. Sinitsa[a], A. M. Solodov[a], R. Barber[b], J. Tennyson[b], and R. N. Tolchenov[b]

[a] *Institute of Atmospheric Optics, Siberian Division, Russian Academy of Sciences, Tomsk, 634055 Russia*
[b] *University College London, WCIE 6BT London, UK*

Received September 24, 2007

Abstract—The shift coefficients for the lines of the $\nu_1 + \nu_2 + \nu_3$ and $\nu_2 + 2\nu_3$ bands of H_2O in the region from 9403 to 9413 cm^{-1} are measured and calculated. The measurements are performed using an intracavity laser spectrometer based on a neodymium laser with a determination error of the line center of 0.003–0.004 cm^{-1}. The Ar, Kr, and Xe noble gases, as well as nitrogen, oxygen, and hydrogen were used as buffer gases. The coefficients of shifts in eight H_2O absorption lines induced by oxygen, nitrogen, and atmospheric air pressures fall into the region from –0.004 to –0.069 cm^{-1}/bar. The calculations are performed by a semiempirical method using variational wave functions, which, in contrast to other studies, correctly takes into account intramolecular interactions. The calculated values agree satisfactorily with experimental data.

PACS numbers: 33.20.-t, 33.20.Vq, 33.70.Jg

DOI: 10.1134/S0030400X08070059

INTRODUCTION

Gas pressure-induced shifts of the centers of vibrational–rotational lines are of considerable interest for investigation of intermolecular interactions in gases. The line shift, in contrast to the line halfwidth, strongly depends on vibrational quantum numbers, and the shift coefficients in the low and highly excited bands may differ in value by an order of magnitude and even have different signs. A strong vibrational effect, which is characteristic of the pressure-induced shift of molecular lines, is caused by the dependence of the intermolecular potential on the vibrational variables of colliding molecules. Thus, the shift coefficients contain important information about molecular interaction forces and their dependences on atomic vibrations. Because of this, much attention in recent years has been paid to the measurements and calculations of these parameters [1–30].

It should be noted that, in this problem, the measured data on the weak absorption lines corresponding to the transitions to high vibrational and rotational states are of great interest. The vibrational effect is especially strong for these lines. However, the profiles of weak lines in the near IR and visible regions are rather difficult to measure by photometric methods. These methods are characterized by using long-base cells and large measurement times, which complicates the measurement process.

The shifts of water vapor lines have been measured using Fourier spectrometers [2–7], diode laser [8–13] and optoacoustic spectrometers [1, 14–17], microwave spectroscopy methods [18, 19], and laser photometry [20–23]. The measurements were performed with a high spectral resolution in wide spectral regions. For example, extensive measurements of broadening and shifts of more than 1000 lines of the ν_2 band that were induced by nitrogen and air pressure were performed in [3]. The results of measurements in the high-frequency region, from 13000 to 26000 cm^{-1}, are presented in [5]. The authors of [14] studied the shift in the H_2O lines induced by the pressure of noble gases, while papers [1, 6, 11, 26–30] present the calculated shifts of water vapor lines induced by the pressure of various buffer gases. The results of numerical calculations have been used to determine the temperature and vibrational dependences, to study the influence of various intramolecular effects, and to develop mass calculation methods. Thus, a large body of data on the shift coefficients for H_2O lines has been obtained to date. It should be noted that the works cited above present not a complete review but only some examples of investigations in the field under discussion.

The method of intracavity (IC) laser spectroscopy, with a modified measurement technique and improved recording instrumentation, opens new possibilities for such investigations.

The method of broadband IC laser spectroscopy [31] is based on the quenching of laser radiation at the frequencies of absorption lines of a substance placed inside the laser cavity. In this case, the spectrum of the laser radiation, recorded by ordinary spectral devices, has sharp dips at the frequencies of the absorption lines.

In the IC laser spectroscopy, the laser is a nonlinear detector of weak absorption. The laser imitates a multipass absorption cell, but with a much longer effective length L_{eff} of the absorbing layer than in ordinary multipass cells, where the effective length is limited by the loss of radiation on mirrors. For quasi-continuous laser radiation with a duration of 1 ms in a cavity completely filled with an absorbing substance, the length L_{eff} may reach 300 km. The IC spectroscopy method is characterized by a high absorption sensitivity (10^{-7}–10^{-9} cm^{-1}), which allows one to record weak absorption lines in high-lying vibrational bands.

In addition to high sensitivity, IC spectroscopy has some other advantages; namely, a wide spectrum (exceeding 100 cm^{-1}) with tens of absorption lines can be recorded during one laser pulse while the small dimensions of the cavity allows one to study substances under external excitation or at high pressures and temperatures. From this point of view, IC spectroscopy is an important additional tool that can considerably extend the possibilities of investigating the relaxation parameters of lines. As an example of application of the IC method, we point out study [32], in which the methane line shift is measured at a low temperature (77 K).

In this study, we determine the shift coefficients of the centers of absorption lines of the (111)–(000) and (012)–(000) vibrational–rotational bands of water vapor induced by the pressure of noble gases (argon, xenon, and krypton), as well as of nitrogen, oxygen, and air. Our calculations performed within the framework of the semiempirical method developed previously in [28–30] are in good agreement with the measured values. A specific feature of the calculations is the use of exact vibrational–rotational wave functions for determination of the strengths of dipole transitions. The wave functions are obtained by direct variational calculations with a highly accurate potential energy function [33, 34].

EXPERIMENTAL

To record the shifts of the centers of absorption lines in the region of 1.06 μm, we used an IC laser spectrometer based on neodymium glass [35]. The spectrometer has the following characteristics: the spectral range is 9380–9460 cm^{-1}, the spectral resolution is 0.035 cm^{-1}, the threshold absorption coefficient sensitivity is 10^{-8} cm^{-1}, and the relative accuracy in determining the line centers is in the range 0.002–0.005 cm^{-1} depending on the line intensities.

The measurement of line centers by IC spectroscopy has a number of sources of errors. The strongest effect on the shift of centers of absorption lines is exerted by variations in the diffraction spectrograph geometry with varying temperature. We experimentally showed that a change in the environmental temperature by one degree noticeably shifts the centers of absorption lines. To control and to take into account such distortions, in addition to direct measurements of the laser radiation spectrum, we performed measurements with the use of an external stabilized interferometer. The developed technique is described in more detail in [36]. As an interferometer, we used a plane-parallel plate made of K8 optical glass without a reflecting layer. The interferometer was placed outside the laser cavity on its axis behind the end mirror, whose transmittance was about 0.01. A portion of the laser radiation that passed through this mirror was reflected from the interferometer and returned into the cavity. Due to the high sensitivity of the IC method, we observed sharp dips in the radiation intensity, spaced by a distance dependent on the interferometer base. For an interferometer 15.5 mm long, the halfwidth of the interference maxima was about 0.04 cm^{-1}. Since the spectral range recorded during one pulse was determined by the length of the CCD array and was 14 cm^{-1}, the IC spectrum simultaneously showed about 70 maxima.

In this study, we estimated the shifts of the interference pattern with varying temperature and showed that, if the interferometer temperature is maintained with an accuracy of 0.02°C, the shift of the interference maxima does not exceed 0.001 cm^{-1} and is not observed within the experimental error. In this case, the shifts of the centers of absorption lines can be detected by the positions of the interference maxima without using additional reference lines.

The measurements were performed for single isolated water vapor absorption lines in the region from 9403 to 9414 cm^{-1} at room temperature at buffer gas pressures of 10–1000 mbar. The pressure was measured by a DVR-25 pressure gauge with an accuracy better than 1%. We used a quartz cell 600 mm long and 10 mm in diameter.

Initially, we measured the laser radiation spectrum in the absence of water vapor (background radiation) and then recorded this spectrum with the interferometer and determined the positions of maxima of the interference pattern. Such measurements were performed for each given pressure of the broadening gas. Since the shift of the spectrum was determined using the positions of the centers of 60–70 maxima, the error in the shift, caused by temperature distortions, was by an order of magnitude smaller than in the case of analyzing single maxima and did not exceed 0.001 cm^{-1}. This correction of the frequency scale was performed after each measurement of the spectra with different pressures of the buffer gas. The next step was to measure the absorption spectrum of pure water vapor at a pressure of 20 mbar. We performed averaging over 30 spectra because the accumulation of the signal allowed us to increase the signal-to-noise ratio. Next, we measured the spectra of the H_2O–buffer gas mixture, also recording 30 spectra.

We determined the shift of the water-vapor absorption line profile in the presence of a buffer gas with respect to the position of the corresponding pure H_2O

absorption line center. The centers of the absorption lines were determined by fitting the theoretical contour to the experimental one by the least squares method. The Lorentz and Voigt profiles were used for approximation. As an example of our measurements of the shift of line centers, Fig. 1 shows the $12_{2\,10}$–$11_{0\,11}$ absorption line of the $\nu_1 + \nu_2 + \nu_3$ band at different argon pressures.

CALCULATION METHOD

The line shift coefficients were calculated by a semiempirical method developed previously in [28, 29] and successfully used for calculation of halfwidths and shifts of lines of water vapor and carbon dioxide [30]. In the semiempirical method, the shift of the line center is represented as the sum

$$\delta_{if} = B(i, f) + \sum_{i'} D^2(ii'|l)P_l(\omega_{ii'}) + \sum_{fi} D^2(ff'|l)P_l(\omega_{ff'}) + \ldots, \tag{1}$$

where

$$B(i, f) = A\frac{n}{c}(\alpha_i - \alpha_f)\sum_{p}\rho(p)\int_0^{\infty} d\mathrm{v}\,\mathrm{v}f(\mathrm{v})b_0^{-3}(\mathrm{v}, i, f, p) \tag{2}$$

is the contribution of the adiabatic part of the interruption function, which is determined by the isotropic part of the intermolecular potential. Here, $b_0(\mathrm{v}, i, f, p)$ is the Anderson interruption radius, A is a known constant [37], α_i and α_f are the polarizabilities of the molecule in the initial and final vibrational states, p denotes the states of the perturbing molecule, $\rho(p)$ is the population of the p level, v is the relative velocity, and $f(\mathrm{v})$ is the Maxwell distribution function.

The sums in (1) include transitions of different types (dipole, quadrupole, etc.) and contain products of two variables, $D^2(ii'|l)$ and $P_l(\omega_{ii'})$. The transition strengths $D^2(ii'|l)$ and $D^2(ff'|l)$ related to the scattering channels $i \longrightarrow i'$ and $f \longrightarrow f'$ depend only on the properties of the absorbing molecule (dipole or quadrupole momenta and wave functions) and involve only intramolecular effects. The terms with $l = 1$ correspond to dipole transitions, while the terms with $l = 2$ correspond to quadrupole transitions in the main molecule.

The coefficients $P_l(\omega_{ii'})$ can be considered to be efficiency functions of the scattering channel $i \longrightarrow i'$ and depend on the properties of the exciting molecule,

$$P_l(\omega) = \frac{n}{c}\sum_{p}\rho(p)\sum_{l',p'}A_{ll'}D^2(pp'|l') \times \int_0^{\infty} d\mathrm{v}\,\mathrm{v}f(\mathrm{v})F_{ll'}\left(\frac{2\pi c b_0(\mathrm{v}, i, f, p)}{\mathrm{v}}(\omega + \omega_{kk'})\right). \tag{3}$$

Here, $A_{ll'}$ are the known constants of Anderson theory, which determine the contribution of the ll' interaction to the interruption function of the second order [37], and $F_{ll'}(x)$ are the resonance functions. The functions $P_l(\omega_{ii'})$ depend on the intermolecular potential, on the trajectory of motion of colliding molecules, and on the energy level structure and wave functions of the perturbing molecule. The $D(ii'|l)$ and $D(ff'|l)$ multipliers can be determined rather accurately, while the intermolecular potential parameters are determined with a lower accuracy. Hence, it seems logical to divide the equation terms into well- and poorly-determined and to correct the latter by introducing a semiempirical factor.

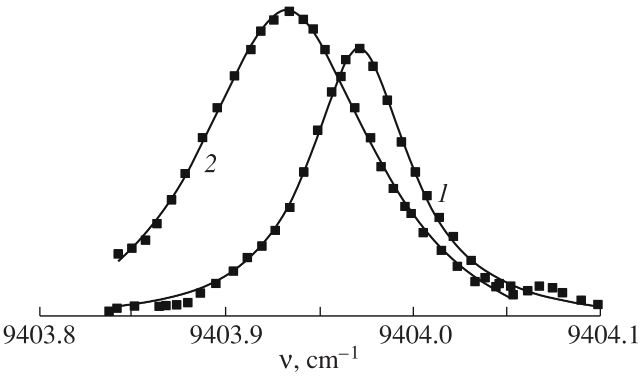

Fig. 1. Experimental profiles of the H_2O absorption line 9403.9716 cm^{-1} ($\nu_1 + \nu_2 + \nu_3$) $12_{2\,10}$–$11_{0\,11}$ at different argon pressures: (*1*) $P_{H_2O} = 21$ mbar and (*2*) $P_{H_2O + Ar} = 882$ mbar.

The term $P_l(\omega_{ii'})$ is a smooth function; therefore, it is reasonable to introduce a correction factor into this function, leaving the terms $D^2(ii'|l)$, which determine the probabilities of transitions in the absorbing molecule, unchanged,

$$P_l(\omega) = C_l(\omega)P_l^A(\omega), \tag{4}$$

where $P_l^A(\omega)$ is the efficiency function in the Anderson approximation [37] and $C_l(\omega)$ is the correcting factor determined from fitting to the experimental parameters of line profiles. The use of the efficiency function $P_l^A(\omega)$ as the main part in Eq. (4) allows us to reproduce the correct behavior of the halfwidths and shifts at large rotational quantum numbers or at high temperatures.

In this study, the line broadenings were calculated using the efficiency functions in the form

$$P_l(\omega_{ff'}) = P_l^A(\omega_{ff'})[c_1/(c_2\sqrt{j_f} + 1)], \tag{5}$$

where c_1 and c_2 are the fitting parameters.

Thus, we used the correcting factor to the $P_l^A(\omega)$ function in the form of a simple expression containing

Table 1. Experimental conditions

P–H_2O, mbar	$P(H_2O + N_2)$, mbar	$P(H_2O + O_2)$, mbar	$P(H_2O + \text{air})$, mbar
21	21	21	21
21	210	217	250
21	425	400	410
21	590	644	640
21	836	870	910

two parameters determined from fitting to experimental data. However, this is not a simple procedure of fitting to an experimental curve because the correcting term, obtained as a result of fitting to several values of broadening coefficients of a band, describes not only the experimental results for this band, but also the broadening and shift of lines for the entire set of the bands of the colliding pair.

For H_2O–N_2 calculations, we used the c_1 and c_2 parameters determined previously in [28–30]. In the other cases, we changed the c_1 parameter. The mean dipole polarizability in the upper vibrational state was determined previously in [28].

In this study, the strengths of dipole transitions were calculated by two methods. In the first method, we used the wave functions of the effective rotational Hamiltonian. The rotational and centrifugal constants of different vibrational states of H_2O were taken from different publications; the resonance mixing of states was neglected. Such an approach is common for calculation of halfwidths and shifts of lines.

In the second method, we used more accurate vibrational–rotational wave functions obtained by the linear variational method with a highly accurate potential energy function [34]. These wave functions, in contrast to the approximate functions used in the first method of calculation, completely take into account all intramolecular interactions. The linear variational method allows one to develop a global method for describing the vibrational–rotational energy spectrum of a molecule and has approximately equal accuracy for the lower and highly excited states.

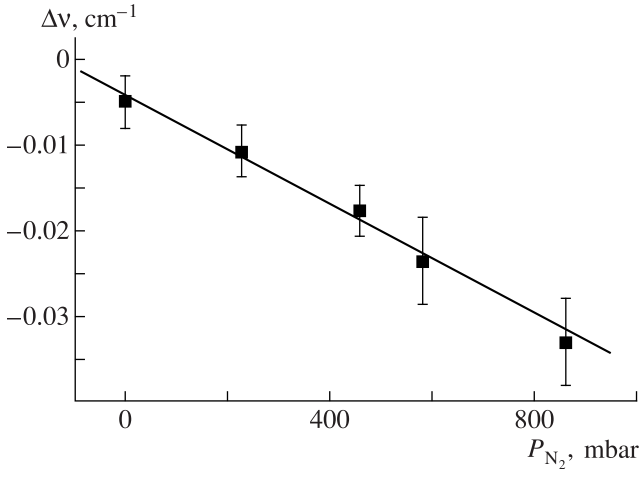

Fig. 2. Dependence of the shift of the center of the 10_{73}–9_{54} absorption line of the (111) band of H_2O on the nitrogen pressure.

Previously [33], the Einstein coefficients for all possible transitions between the states with energies up to 30000 cm^{-1} were calculated and included in the BT2 line list. These data from BT2 were used in our calculations of the halfwidths and shifts of lines for transitions in the region of 1.06 μm.

RESULTS AND DISCUSSION

In this study, we determined the shifts coefficients of the centers of eight water vapor absorption lines, induced by the pressure of nitrogen, oxygen, dehydrated atmospheric air, and noble gases (argon, xenon, and krypton). Table 1 shows the conditions of these measurements.

The shift coefficients of H_2O lines for each buffer gas were determined in a series of five measurements with the buffer gas pressures varied from 0 to 1000 mbar. As an example, Fig. 2 shows the dependence $\Delta\nu(P)$ for the 10_{73}–9_{54} line of the (111) band of H_2O. Note that this dependence is linear. To check the measurement method, these series were repeated three times or more. The reproducibility of the results was very good, the difference between the results obtained in different series was comparable with the error for individual series of measurements. To eliminate the effect of the shift induced by the pressure of water vapor itself, all measurements of a series were performed at the same partial pressure of water vapor.

The measurements were performed for the absorption lines of the $\nu_1 + \nu_2 + \nu_3$ and $\nu_2 + 2\nu_3$ vibrational–rotational bands in the region from 9403 to 9414 cm^{-1}. Table 2 presents the measured centers of lines, the quantum identification, and the coefficients of the shift of the centers of absorption lines. The dependence of the shift of line centers on the buffer gas pressure was linear for all the absorption lines. The shift coefficients varied from –0.004 to –0.029 cm^{-1}/bar. It should be emphasized that the measurements were performed for very weak lines of H_2O, which correspond to the transitions to the states with quantum numbers $J = 8$–12 and $K_a = 2$–8 and whose intensities range from 1.4×10^{-25} (for the strong line (012) 8_{36}–7_{07}) to 2.28×10^{-26} cm/mol (for the weak line (012) 10_{74}–9_{63}).

The seventh column of Table 2 lists the measured coefficients δ_{exp} of shift of the absorption line centers, induced by atmospheric air pressure, and the coefficients δ calculated according to the partial content of oxygen and nitrogen in air and using the data from col-

Table 2. Measured coefficients of shifts of the centers of H_2O lines, induced by nitrogen, oxygen, and air pressures ($T = 300$ K)

Frequency, cm^{-1}	$V_1V_2V_3$	$JK'_aK'_c$	$JK''_aK''_c$	δ_{exp}, $\delta 1_{calc}$, $\delta 2_{calc}$, cm^{-1}/bar (oxygen)	δ_{exp}, $\delta 1_{calc}$, $\delta 2_{calc}$, cm^{-1}/bar (nitrogen)	δ_{exp}, δ, cm^{-1}/bar (air)	Mixing coefficient, %
9403.971	111	12 2 10	11 0 11	−0.0237(30)	−0.0218(35)	−0.0240(40)	7
				−0.028	−0.027	−0.021	
				−0.027	−0.025		
9406.764	012	11 5 6	10 4 7	−0.0129(25)	<0.004	<0.004	25
				−0.022	0		
				−0.017	−0.0012		
9407.258	111	10 7 3	9 5 4	−0.0270(40)	−0.0245(40)	−0.0240(40)	41
				−0.018	−0.021	−0.024	
				−0.027	−0.021		
9409.129	012	8 3 6	7 0 7	−0.0306(40)	−0.0070(30)	−0.0126(30)	2
				−0.027	−0.013	−0.01	
				−0.022	−0.011		
9409.740	111	10 7 4	9 5 5	−0.0320(40)	−0.0204(40)	−0.0231(40)	42
				−0.022	−0.02	−0.022	
				−0.027	−0.02		
9411.416	012	9 8 2	8 7 1	−0.0265(35)	−0.0287(30)	−0.0291(35)	16
		9 8 1	8 7 2	−0.031	−0.03	−0.027	
				−0.0289	−0.026		
9412.407	012	10 7 4	9 6 3	−0.0200(35)	−0.0208(30)	−0.0204(30)	27
				−0.031	−0.022	−0.02	
				−0.028	−0.023		
9412.789	012	8 4 5	7 1 6	−0.0230(40)	<0.004	−0.0070(30)	4
				−0.021	0		
				−0.014	−0.002		

Note: The errors in the last decimal place are shown in parentheses. $\delta = 0.78\,\delta_{N_2} + 0.21\,\delta_{O_2}$.

umns 5 and 6. Comparison of these values shows a good agreement between δ_{exp} and δ for each H_2O absorption line within the measurement error. This additionally confirms the correctness of the measurement method.

The coefficients of shifts of line centers, induced by N_2 and O_2 pressures, were calculated by two methods. The calculations by the first method were performed within the framework of traditional approximations, which incompletely take into account the vibrational–rotational interaction and the vibrational dependence of the line strength $D(ff'|l)$. In the second method, we used probabilities of dipole transitions obtained by highly accurate variational calculations [33].

To demonstrate the role of the vibrational–rotational interaction in calculations of the shift coefficients for H_2O lines, the last column of Table 2 presents the total mixing coefficients, which determine the strength of the resonance effect. One can see a pronounced correlation between the values of the mixing coefficients and the difference between the experimental and calculated $\delta 1_{calc}$ shift coefficients. This correlation is also demonstrated in Fig. 3.

The lines considered belong to transitions to the states of the second hexade, which are characterized by a substantial resonance mixing. The resonance effect is stronger for the states with higher angular momentum quantum numbers. Hence, it is necessary to use more precise wave functions to calculate the collision-induced transitions.

The use of variational wave functions, which take into account the vibrational effect more accurately, yields much better average agreement with experiment. In particular, the mean-root-square deviation of calculation from experiment (in the case of oxygen-induced broadening) is 8×10^{-3} cm^{-1}/bar for the calculation with effective Hamiltonian wave functions and 6×10^{-3} cm^{-1}/bar for calculations using the line strengths from BT-2. For

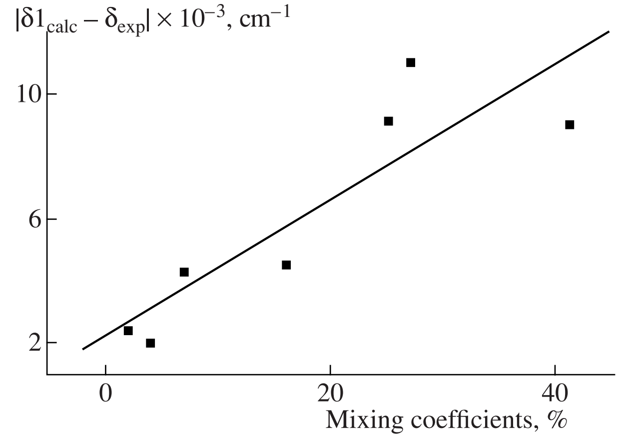

Fig. 3. Correlation between the differences $|\delta1_{calc} - \delta_{exp}|$ and the coefficients of resonance mixing of states.

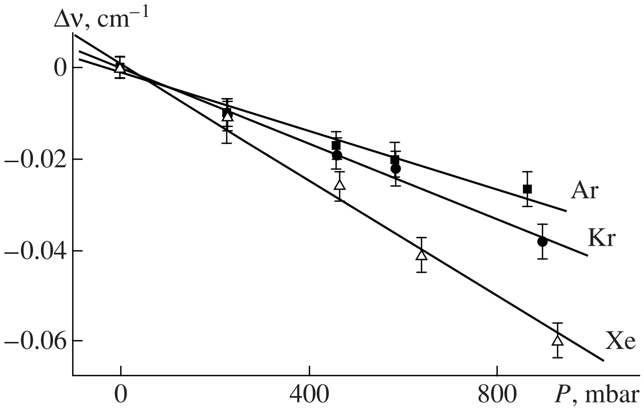

Fig. 4. Dependences of the shift of the center of the 12_{210}–11_{011} absorption line of the (111) band of H_2O on the argon, krypton, and xenon pressures.

all lines, except for two lines centered at 9409.129 and 9412.789 cm^{-1}, the calculations with variational wave functions result in a better agreement with the measured values. A similar pattern is observed for nitrogen- and air-induces broadening.

The coefficients of shifts of line centers induced by the pressure of Ar, Kr, and Xe (Fig. 4), which are characterized by different polarizabilities, are listed in Table 3. The coefficient of shifts of line centers in the region of 1.06 μm, induced by the pressure of noble gases, exceed the sifts coefficients for N_2 and O_2 pressures and reach –0.069 cm^{-1}/bar (for the line at 9411.416 cm^{-1}). Larger shifts were only observed in the case of the self-broadening of H_2O lines [20]. The measured coefficients of shifts of the centers of H_2O lines induced by pressures of noble gases show almost linear dependence on polarizability. This is explained by relation (2), in which the first-order contribution contains the differences between the mean polarizabilities of the excited and ground vibrational states.

Agreement between the experimental and calculated coefficients of shifts induced by pressure of noble gases is somewhat worse. This is obviously caused by insufficiently accurate account for the polarization potential in calculation of the second-order contribution in (1).

Table 3. Measured coefficients of shifts of the centers of H_2O lines, induced by argon, krypton, and xenon ($T = 300$ K)

Frequency, cm^{-1}	$V_1V_2V_3$	$JK'_aK'_c$	$JK''_aK''_c$	δ_{exp}, δ_{calc}, cm^{-1}/bar (argon)	δ_{exp}, δ_{calc}, cm^{-1}/bar (krypton)	δ_{exp}, δ_{calc}, cm^{-1}/bar (xenon)
9403.971	111	12 2 10	11 0 11	−0.0320(30)	−0.0439(30)	−0.0685(40)
				−0.035	−0.045	−0.055
9406.764	012	11 5 6	10 4 7	−0.0306(40)	−0.0468(30)	−0.0505(35)
				−0.029	−0.044	−0.052
9407.258	111	10 7 3	9 5 4	−0.0294(30)	−0.0510(30)	−0.0575(30)
				−0.034	−0.055	−0.067
9409.129	012	8 3 6	7 0 7	−0.0500(45)	−0.0550(40)	−0.0665(30)
				−0.030	−0.040	−0.048
9411.416	012	9 8 2	8 7 1	−0.0326(40)	−0.0513(30)	−0.0699(30)
		9 8 1	8 7 2	−0.032	−0.054	−0.067
9412.407	012	10 7 4	9 6 3	−0.0292(40)	−0.0375(30)	−0.0499(40)
				−0.033	−0.056	−0.069
9412.789	012	8 4 5	7 1 6	−0.0417(40)	−0.0576(40)	−0.0628(50)
				−0.029	−0.033	−0.044

CONCLUSIONS

We presented the results of measurements and calculations of the coefficients of shifts of the centers of weak absorption lines of H_2O in the region of 1.06 μm. As buffer gases, we used Ar, Kr, and Xe noble gases, as well as nitrogen, oxygen, and air. The measurements were performed by the intracavity method with the error in determination of line centers of 0.003–0.004 cm^{-1}. In contrast to other studies, our calculations using a semiempirical method with variational wave functions accurately take into account the intramolecular interactions.

The results obtained show that the measurements by the highly sensitive method of intracavity laser spectroscopy allow one to study the effect of intramolecular interactions in highly excited vibrational–rotational states on the shift of line centers in sufficient detail. The calculations performed demonstrate that intramolecular interactions should be more completely taken into account when calculating the coefficients of pressure-induced shifts of line centers.

ACKNOWLEDGMENTS

This study was supported by INTAS, grant no. 03-51-3394.

REFERENCES

1. W. E. Browell, B. E. Grossman, A. D. Bykov, et al., Opt. Atmos. Okeana **3** (7), 675 (1990).
2. R. A. Toth, L. R. Brown, and C. Plymate, J. Quant. Spectrosc. Radiat. Transfer **59** (6), 529 (1998).
3. R. A. Toth, J. Mol. Spectrosc. **201**, 218 (2000).
4. C. Claveau, A. Henry, D. Hurtmans, and A. Valentin, J. Quant. Spectrosc. Radiat. Transfer **68** (3), 273 (2001).
5. S. Fally, P.-F. Coheur, M. Carleer, et al., J. Quant. Spectrosc. Radiat. Transfer **82**, 119 (2003).
6. R. Lynch, R. R. Gamache, and L. R. Brown, J. Quant. Spectrosc. Radiat. Transfer **56**, 471 (1996).
7. T. Geisen, R. Schieder, G. Winnewisser, and K. M. T. Yamada, J. Mol. Spectrosc. **153**, 406 (1992).
8. V. G. Avetisov, A. I. Nadezhdinskii, A. N. Khusnutdinov, et al., J. Mol. Spectrosc. **160** (2), 326 (1993).
9. A. I. Nadezhdinskii, Spectroch. Acta A **52**, 1041 (1996).
10. J.-M. Hartman, J. Taine, J. Bonamy, et al., J. Chem. Phys. **86** (1), 144 (1987).
11. N. N. Lavrent'eva and A. M. Solodov, Opt. Spektrosk. **98**, 917 (2005).
12. V. Zéninari, B. Parvitte, D. Courtois, et al., Mol. Phys. **102**, 1697 (2004).
13. A. Bandyopadhyay, B. Ray, P. N. Ghosh, et al., J. Mol. Spectrosc. **242**, 10 (2007).
14. A. D. Bykov, V. V. Lazarev, Yu. N. Ponomarev, et al., Opt. Atmos. Okeana **7** (9), 1207 (1994).
15. J. Bsenberg, Appl. Opt. **24** (21), 3531 (1985).
16. Yu. N. Ponomarev and B. A. Tikhomirov, Opt. Spectrosk. **58** (8), 947 (1985).
17. A. D. Bykov, E. A. Korotchenko, Yu. S. Makushkin, et al., Opt. Atmos. **1** (1), 40 (1988).
18. M. A. Koshelev, M. Yu. Tretyakov, G. Yu. Golubiatnikov, et al., J. Mol. Spectrosc. **241**, 101 (2007).
19. S. P. Belov, A. F. Krupnov, V. N. Markov, et al., J. Mol. Spectrosc. **101** (2), 258 (1983).
20. B. E. Grossman and E. V. Browell, J. Mol. Spectrosc. **136**, 264 (1989).
21. B. E. Grossman and E. V. Browell, J. Mol. Spectrosc. **138**, 562 (1989).
22. B. E. Grossman and E. V. Browell, J. Quant. Spectrosc. Radiat. Transfer **45** (6), 339 (1991).
23. B. E. Grossman and E. V. Browell, J. Mol. Spectrosc. **185**, 58 (1997).
24. D. Jacquemart, R. Gamache, and L. S. Rothman, J. Quant. Spectrosc. Radiat. Transfer **96**, 205 (2005).
25. B. K. Antony, S. Neshyba, and R. R. Gamache, J. Quant. Spectrosc. Radiat. Transfer **105**, 148 (2007).
26. R. R. Gamache and J.-M. Hartmann, J. Quant. Spectrosc. Radiat. Transfer **83**, 119 (2004).
27. R. Lynch, R. R. Gamache, and S. P. Neshyba, J. Quant. Spectrosc. Radiat. Transfer **59**, 615 (1998).
28. A. Bykov, N. Lavrentieva, and L. Sinitsa, Mol. Phys. **102**, 1706 (2004).
29. N. N. Lavrent'eva, Opt. Spektrosk. **96** (2), 247 (2004).
30. N. N. Lavrent'eva, in *Optical Spectroscopy and Frequency Standards: Molecular Spectroscopy*, Ed. by L. N. Sinitsyn and E. A. Vinogradov (Institut Optiki Atmosfery, Tomsk, 2004) [in Russian].
31. L. A. Pakhomycheva, É. A. Sviridenkov, and A. F. Suchkov, Pis'ma Zh. Éksp. Teor. Fiz. **12**, 60 (1970).
32. K. Singh and J. J. O'Brien, J. Quant. Spectrosc. Radiat. Transfer **52** (1), 75 (1994).
33. R. J. Barber, J. Tennyson, G. J. Harris, and R. N. Tolchenov, Mon. Not. R. Astron. Soc. **368**, 1087 (2006).
34. G. J. Harris and J. Tennyson, J. Chem. Phys. **117**, 11239 (2002).
35. T. M. Petrova, Yu. Poplavskii, V. Serdyukov, and L. N. Sinitsa, Mol. Phys. **104**, 2691 (2006).
36. T. M. Petrova, L. N. Sinitsa, and A. M. Solodov, Opt. Atmos. Okeana **20** (9), 821 (2007).
37. C. J. Tsao and B. Curnutte, J. Quant. Spectrosc. Radiat. Transfer **2** (1), 41 (1961).

Translated by M. Basieva